Interference of a four-hole aperture for on-chip quantitative two-dimensional differential phase imaging

Matthew Lew,* Xiquan Cui, Xin Heng, and Changhuei Yang

Department of Electrical Engineering, California Institute of Technology, MC 136-93, Pasadena, California 91125, USA

**Corresponding author: mlew@its.caltech.edu*

Received July 18, 2007; revised September 7, 2007; accepted September 8, 2007; posted September 11, 2007 (Doc. ID 85454); published October 5, 2007

We present a novel on-chip method for quantitative two-dimensional differential phase imaging. This technique uses four circular holes (600 nm diameter, 1.2 μm spacing) arranged in a "plus" pattern that are fabricated in a layer of metal above a complementary metal-oxide semiconductor (CMOS) imaging sensor. The interference pattern of the aperture shifts position with respect to the differential phase of the incident light. By imaging the interference pattern with the CMOS sensor, this method measures amplitude and differential phase (1°/μm sensitivity for signal-to-noise ratio $\geq$16 dB) of the incident light field simultaneously. An application to optical beam profiling is presented; we show the amplitude and differential phase profiles of a Gaussian laser beam and an optical vortex.

OCIS codes: 050.1220, 120.5050, 230.3990, 040.6070.

A chip-based high-resolution ($\sim$1 μm) optical phase imaging device can dramatically simplify a broad range of applications, such as beam profiling, phase microscopy, and optical wavefront sensing. In addition to the potential compactness advantage, employing such a device can provide cost savings if it can be manufactured using established chip fabrication techniques and designed to contain few or no optical elements. A review of existing phase imaging techniques will quickly reveal that most of them cannot be translated into high-resolution on-chip versions without significant obstacles or design issues. For example, the Shack–Hartmann wavefront sensor [1] requires the use of optical lenses, which cannot be easily miniaturized to the desired scale of $\sim$1 μm for high-resolution on-chip imaging. Likewise, phase contrast [2] and differential interference contrast [3] microscopy techniques require complicated optical arrangements that are difficult to miniaturize.

In this Letter, we report a novel high-resolution phase imaging method based on measuring the interference pattern of a four-hole aperture fabricated on top of an image sensor chip. The amplitude and spatial differential phase of the light field on the four-hole aperture can be calculated from the amplitude and position of the zero-order fringe. A complete and quantitative phase image of an incident light field can thus be profiled by raster scanning the four-hole aperture over the light field. The number of sensor pixels required per four-hole aperture for accurate measurement is surprisingly small ($\sim$15 pixels $\times$15 pixels). As such, multiple four-hole apertures can be implemented on the same chip to parallelize image acquisition and simplify the scanning process via approaches such as a slanted hole array beam profiler (SHArP) [4]. In the next section, we describe the geometry of our device in detail. Then, we derive a relationship between spatial differential phase and position of the zero-order fringe and verify this relationship experimentally. We also show that our device achieves 1°/μm differential phase sensitivity for a signal-to-noise ratio (SNR) as low as 16 dB. Finally, we demonstrate our device in a beam-profiling application by imaging a Gaussian laser beam and an optical vortex.

The geometry of our device and its principle of operation are shown in Fig. 1(a). We use a 10-bit grayscale complementary metal-oxide semiconductor (CMOS) image sensor (Micron MT9V403) with 9.9 μm $\times$ 9.9 μm pixels as the substrate for an 80 μm

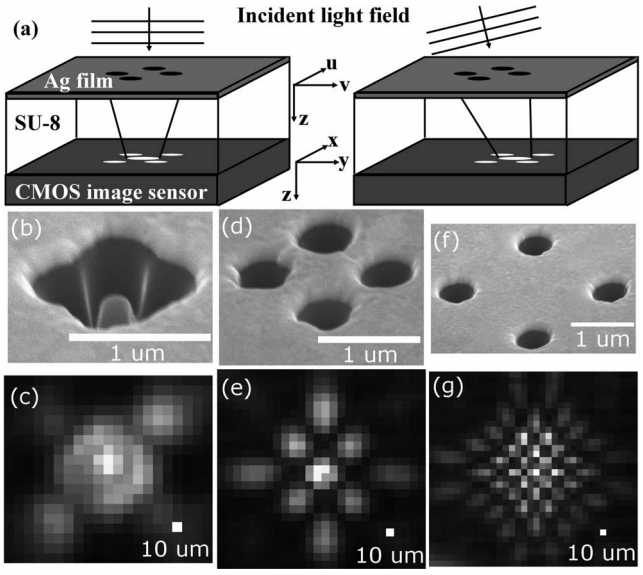

Fig. 1. (a) Device geometry and principle. (b) SEM image and (c) interference pattern of 600 nm holes with 600 nm spacing. (d), (e) Same plots for holes with 1.2 μm spacing. (f), (g) Same plots for holes with 2.4 μm spacing.

0146-9592/07/202963-3/$15.00

thick layer of SU-8. We then evaporate a 100 nm thick layer of silver on top of the SU-8 and use a focused ion beam (FEI Company Nova 200 NanoLab) to mill four circular holes, 600 nm in diameter, into the silver. Various values were used for the center-to-center distance between the holes, including 600 nm, 1.2 μm, and 2.4 μm. The light transmitted through the holes interacts to project an interference pattern onto the sensor. Scanning electron microscope (SEM) images of the four-hole apertures and images of their corresponding interference patterns are shown in Figs. 1(b)–1(g). As shown in Fig. 1(e), the size of the principal interference pattern (zero and first orders) for holes with 1.2 μm spacing is only 15×15 pixels.

Similar to the analysis of Young's double-slit experiment, we use geometrical optics to predict the relationship between the spatial differential phase $\partial\phi(u,v)/\partial u$ of the light field and the position of the zero-order fringe $x_{\text{zerofringe}}$ [see Fig. 1(a) for coordinate system definition]. We assume that the incident angle of the light field on our aperture is the same as the transmission angle. We find that

$$x_{\text{zerofringe}} = d\tan\left[\arcsin\left(\frac{\lambda}{2\pi}\frac{\partial\phi}{\partial u}\right)\right], \tag{1}$$

where d is the distance between the aperture and the image sensor and λ is the wavelength of the light field. A similar equation can be derived for $y_{\text{zerofringe}}$. From Eq. (1), we can see that responsivity favors large distance. However, the distance between aperture and image sensor is inversely proportional to the fringe intensity on the image sensor, imposing a trade-off between responsivity and signal strength. Using a collimated He–Ne laser beam (632.8 nm wavelength, 4.2 mm spot diameter, 2 mW intensity) to illuminate our device, which was mounted on a two-axis goniometer (Thorlabs GN2), we experimentally verified Eq. (1). The goniometer was used to alter the incident angle of the laser beam along the u and v directions, and the translation of the fringes was mapped for several incidence angles (see Fig. 2). In our experiments, $x_{\text{zerofringe}}$ and $y_{\text{zerofringe}}$ were determined by fitting the measured zero-order fringe to a 2D Gaussian profile. The measured values were fit to a linearization of Eq. (1) for calibration purposes; for our device parameters ($d=80$ μm, $\lambda=632.8$ nm), Eq. (1) fits to a linear curve with an R-square value of 0.995 for $|\partial\phi(u,v)/\partial u|\le 360°/\mu$m. Experimentally, the optimum hole separation was found to be 1.2 μm, as it is the best combination of fringe size and fabrication quality to our knowledge.

In principle, a differential phase profiler can also be created by using a single hole as the aperture, similar to Hartmann's perforated screen [5]. The diffraction pattern associated with such an aperture exhibits a similar zero-order lobe that obeys Eq. (1). However, the lobe is significantly wider than that of a similar-sized four-hole aperture, leading to a larger variation in the experimental determination of lobe location. For example, the zero-order lobe of a 1.2 μm diameter hole is 80% wider than that of our device's four-hole aperture. In simulations that account for shot noise, the phase sensitivity of a single-hole aperture is 20% worse than that of a four-hole aperture. In addition, the behavior of the single-hole aperture deviates from Eq. (1) as the hole becomes smaller than one wavelength [6], effectively rendering it less useful for high-resolution differential phase imaging.

Characterizing the noise in our device is crucial in determining its differential phase sensitivity. The measurement was performed by projecting a He–Ne laser beam (1.8 mm spot diameter, 4 mW intensity) on our device and taking many snapshots of the interference pattern for various exposure times. Ideally, our device should give identical differential phase measurements for every snapshot regardless of exposure time, but noise in our system prevents this. Signal power is defined here as the intensity of the interference pattern averaged over snapshots with identical exposure time. Noise power is defined as the standard deviation of the intensity over snapshots with identical exposure time. The standard deviation of the calculated differential phase is defined as the sensitivity of our device, shown in Fig. 3. Notice that $1°/\mu$m phase sensitivity is achieved for a SNR as low as 16 dB. Any data whose SNR is below 16 dB was discarded in the following measurements.

To demonstrate phase imaging, we projected a collimated He–Ne laser beam (4.2 mm spot diameter, 2 mW intensity) through an aspheric lens (Thorlabs C220TME-B, 11 mm focal length) focused ahead of the device (i.e., $z>0$). This creates a differential phase pattern given by

$$\nabla\phi_{\text{Gauss}}(u,v,z) = \frac{\partial\phi_{\text{Gauss}}}{\partial u}\hat{u} + \frac{\partial\phi_{\text{Gauss}}}{\partial v}\hat{v} = \frac{ku}{z[1+(z_0/z)^2]}\hat{u} + \frac{kv}{z[1+(z_0/z)^2]}\hat{v}, \tag{2}$$

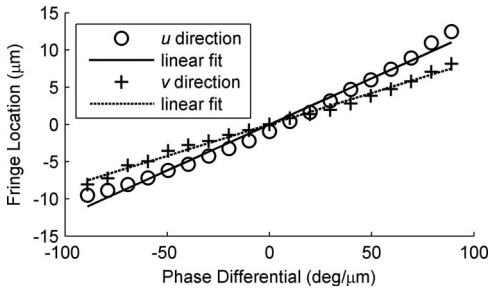

Fig. 2. Device responsivity.

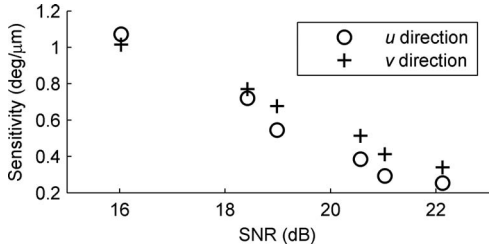

Fig. 3. Device phase sensitivity.

where $k=2\pi/\lambda$, $z_0=\pi w_0^2/\lambda$, and w_0 is the minimum waist radius of the beam. Our device was raster scanned by a motorized (Newport CMA-25CCCL) two-axis precision translation stage controlled by a Newport ESP-300 motor controller. The motor controller and camera were coordinated by custom computer software to automate raster scanning and snapshot routines. The amplitude and differential phase profiles of the Gaussian beam are shown in Figs. 4(a)–4(d). Note that crosstalk between amplitude and differential phase measurements in Figs. 4(a)–4(c) is virtually nonexistent. Thus, our device does not need a uniform intensity distribution in order to accurately measure differential phase.

Next, we used a computer-generated hologram to generate an optical vortex [7] of topological charge one to image with our device. The interference pattern of a plane wave and an optical vortex at a 2° incidence angle was computed and used as the pattern for a chrome mask. A collimated He–Ne laser beam (2 mW intensity) was projected onto the hologram,

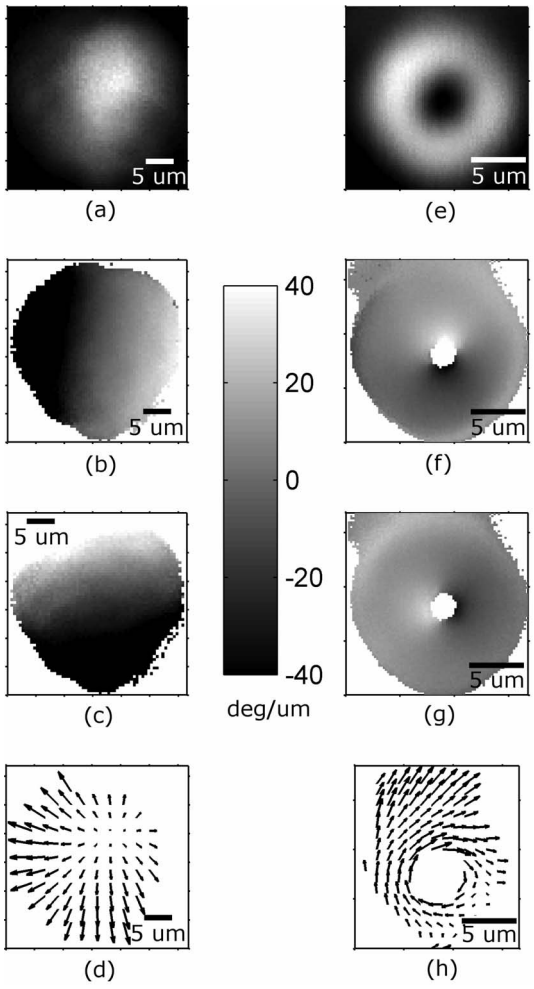

Fig. 4. (a) Intensity, (b) u component and (c) v component of differential phase, and (d) vector representation of differential phase of a Gaussian beam. (e)–(h) Same plots for an optical vortex.

and the first-order diffraction component (3.9 mm spot diameter) was focused onto our device (i.e., $z=0$) by a plano-convex lens (Thorlabs LA1951, 25.4 mm focal length). This creates a differential phase pattern given by

$$\nabla\phi_{\text{vortex}}(u,v,z=0)=-\frac{mv}{u^2+v^2}\hat{u}+\frac{mu}{u^2+v^2}\hat{v}, \qquad (3)$$

where m is a signed integer called the topological charge. Our device was scanned across the vortex to measure its amplitude and differential phase profiles, which are shown in Figs. 4(e)–4(h). The differential phase of the vortex rotates about the center and is larger near the center, as predicted by Eq. (3). The experimentally measured line integral around the vortex in the $\hat{\theta}$ direction equals 332° with a standard deviation of 3.71° for radii between 2 and 4 μm.

In conclusion, we have demonstrated a novel on-chip device for high-resolution phase imaging that utilizes the interference pattern of a four-hole aperture. This device can be fabricated with existing lithographic techniques and contains no optical elements, making it an inexpensive, readily implementable alternative to current phase imaging methods. Since the number of sensor pixels required to capture the interference pattern of the four-hole aperture is small, a slanted 1D array or 2D array of four-hole apertures can be employed to parallelize the scanning process, much like SHArP [4]. Furthermore, a microfluidic channel could be fabricated on top of this array to efficiently scan biological cells, creating a phase-sensitive optofluidic microscope [8]. One weakness of our device is that it is intrinsically lossy since we are sampling the light field of interest with small holes. This was not an issue in our experiments, but using stronger illumination or more sensitive imaging sensors can compensate for this loss.

The authors acknowledge financial support from the Defense Advanced Research Projects Agency Center for Optofluidic Integration. We thank S. Han, J. Wu, and Z. Yaqoob for their technical assistance and enlightening discussions.

References

1. J. Z. Liang, B. Grimm, S. Goelz, and J. F. Bille, J. Opt. Soc. Am. A **11**, 1949 (1994).
2. M. Pluta, Opt. Eng. **32**, 3199 (1993).
3. M. R. Arnison, K. G. Larkin, C. J. R. Sheppard, N. I. Smith, and C. J. Cogswell, J. Microsc. **214**, 7 (2004).
4. X. Q. Cui, X. Heng, J. G. Wu, Z. Yaqoob, A. Scherer, D. Psaltis, and C. H. Yang, Opt. Lett. **31**, 3161 (2006).
5. J. Hartmann, Astrophys. J. **12**, 30 (1900).
6. X. Heng, X. Q. Cui, D. W. Knapp, J. G. Wu, Z. Yaqoob, E. J. McDowell, D. Psaltis, and C. H. Yang, Opt. Express **14**, 10410 (2006).
7. Z. S. Sacks, D. Rozas, and G. A. Swartzlander, J. Opt. Soc. Am. B **15**, 2226 (1998).
8. X. Heng, D. Erickson, L. R. Baugh, Z. Yaqoob, P. W. Sternberg, D. Psaltis, and C. H. Yang, Lab Chip **6**, 1274 (2006).